Substrate Channeling Hot Paper

Krebs Cycle Metabolon: Structural Evidence of Substrate Channeling Revealed by Cross-Linking and Mass Spectrometry**

*Fei Wu and Shelley Minteer**

Abstract: *It has been hypothesized that the high metabolic flux in the mitochondria is due to the self-assembly of enzyme supercomplexes (called metabolons) that channel substrates from one enzyme to another, but there has been no experimental confirmation of this structure or the channeling. A structural investigation of enzyme organization within the Krebs cycle metabolon was accomplished by in vivo cross-linking and mass spectrometry. Eight Krebs cycle enzyme components were isolated upon chemical fixation, and interfacial residues between mitochondrial malate dehydrogenase, citrate synthase, and aconitase were identified. Using constraint protein docking, a low-resolution structure for the three-enzyme complex was achieved, as well as the two-fold symmetric octamer. Surface analysis showed formation of electrostatic channeling upon protein–protein association, which is the first structural evidence of substrate channeling in the Krebs cycle metabolon.*

The Krebs cycle, also known as the tricarboxylic acid cycle, plays an essential role in maintaining life functions in cells, by completely oxidizing biofuels transformed to acetyl Coenzyme A and generating reducing power (NADH) for ATP production.[1] Srere et al. postulated that the eight Krebs cycle enzymes, mitochondrial malate dehydrogenase (mMDH), citrate synthase (CS), aconitase (ACON), iso-citrate dehydrogenase (ICDH), α-ketoglutarate dehydrogenase complex (KDH), succinyl-CoA synthetase (SCS), succinate dehydrogenase (SDH), and fumarase (FUM), form a supramolecular complex, termed a metabolon, through weak non-covalent interactions.[2] It was proposed that organization of these enzymes allows efficient intermediate transport between active sites and improves sequential catalytic performance.[2c,3] This proposal has attracted increasing attention of researchers in the field of enzymatic biofuel cells using

enzyme cascade as bioelectrocatalyst, as well as researchers focusing on cell-free biotransformations. Substrate channeling will enhance mass transport and improve the rate of energy conversion in an enzyme cascade. The Minteer group first applied crude mitochondrial lysate containing cross-linked Krebs cycle metabolons on the anode of a pyruvate/air biofuel cell, and achieved impressive improvement in both current and power densities.[4]

Although efforts have been made to assemble enzyme cascades into complexes as metabolon biomimics,[5] there is little knowledge of enzyme–enzyme interactions in natural metabolons, because they dissociate upon disturbance of the intracellular environment during isolation and purification. With the help of protein engineering and computer modeling, Srere and co-workers proposed a symmetric model for mMDH-CS-ACON complex as a part of the complete Krebs cycle metabolon, in which two N-termini of the mMDH homodimer were fused to the two C-termini of the CS homodimer, whose N-terminus was in turn fused to the C-terminus of two ACON monomers. With this intelligent structure, they managed to illustrate, by numerical simulation, a continuous surface region of positive potential that could direct efficient substrate channeling.[3c,6] With the great advances in mass spectrometry in proteomic studies, it is possible to experimentally probe the native structure of in vivo protein–protein networks, for which high-resolution techniques, such as X-ray crystallography are not feasible.[7] Herein, we combine in vivo chemical cross-linking (XL) and mass spectrometry (MS) to identify interfacial residues in the mMDH-CS-ACON complex. With distance constraints obtained from XL-MS experiments, we establish a low-resolution structure for the mMDH-CS-ACON complex using a hybrid protein docking method and compare this structure to Srere's predicted structure.

To explore protein–protein interactions in the Krebs cycle by XL-MS, a bottom-up approach was used. Intact mitochondria isolated from fresh beef heart were treated with disuccinimidyl glutarate (DSG) to fix matrix protein complexes, which were finally separated by reducing SDS-PAGE by molecular mass. Compared to the non-cross-linked sample, additional intense protein bands appeared at the top of the gel after cross-linking, indicating generation of protein complexes of high molecular weight (Figure S1 in the Supporting Information). Assuming that the Krebs cycle metabolon has a molecular weight over 8000 kDa,[8] we cut the band just near the well of the lane to which the cross-linked sample was applied,[9] and digested proteins inside the gel band with trypsin, which specifically cuts amide bonds at the C-terminus of lysine or arginine residues. Tryptic peptides were further fractionated and analyzed by liquid chromatography–tandem

[*] F. Wu, Prof. S. D. Minteer
Chemistry Department
University of Utah
315 S1400 E, Salt Lake City, UT 84112 (USA)
E-mail: minteer@chem.utah.edu

mass spectrometry (LC-MS/MS) for protein and cross-link identification. As the native control, the top band as well as individual enzyme bands in the non-cross-linked lane was also cut for trypsin digestion and mass spectrometry analysis.

As listed in Table 1, only mMDH and CS were present in the non-cross-linked band, indicating dissociation of the

***Table 1:*** Identified Krebs cycle enzymes in native and DSG-cross-linked bands.

Sample	Enzyme	Mass (Da)	Peptides matched[a]
Native	mMDH	33 061	4
	CS	51 673	2
Cross-linked	mMDH	33 061	33
	ACON	85 304	14
	CS	51 673	13
	ICDH	50 792	11
	SCS	46 774	3
	KDH	48 554	2
	FUM	49 978	1
	SDH	72 280	1

[a] Mass error tolerance is 5 ppm.

metabolon, but a strong interaction between these two enzymes. After chemical fixation by DSG, all Krebs cycle enzyme components were identified with at least one tryptic peptide matching database. This confirms the existence of the metabolon. It is worth mentioning that SDH is also Complex II of the electron-transport chain in the inner mitochondrial membrane and may anchor the rest of the Krebs cycle to the surface of the inner mitochondrial membrane.[10] Cross-linking of SDH to its nearby enzymes in the Krebs cycle and to the electron-transport chain, caused their co-precipitation with membrane fractions during centrifugation and ammonium sulfate precipitation. This process explains significant loss of tryptic peptides in SDH, FUM, SCS, and KDH. According to the supramolecular model of the Krebs cycle metabolon proposed by Lyubarev and Kurganov, the KDH complex acts as the nucleus surrounded by SCS and FUM, followed by assembly of mMDH, CS, ACON, and ICDH at the outer shell.[8] Trypsin digestion might be inefficient in the core of the giant complex, causing missed detection of enzyme peptides.

To model the structure of the mMDH-CS-ACON complex based on XL-MS results, lysine residues within cross-linking distance (25 Å) were determined and summarized in Figure S2. Given these distance constraints, a hybrid docking method was utilized to model protein–protein interactions in a rational fashion (Figure S3). Detailed description of the cross-link identification and protein docking is available in the Supporting Information.

CS homodimer, the biggest of the three enzymes, was set as the receptor during modelling. Prior to docking ACON, mMDH was allowed to explore the whole surface of CS until a model was found to satisfy our distance requirement. As shown in Figure 1, mMDH-CS complex turned out to be asymmetric with only one subunit of each dimer involved in protein–protein interaction, which is quite different from Srere's symmetric fusion protein. Three cross-links were
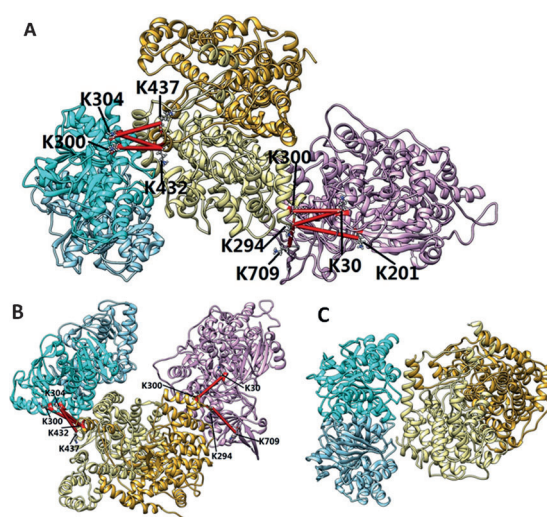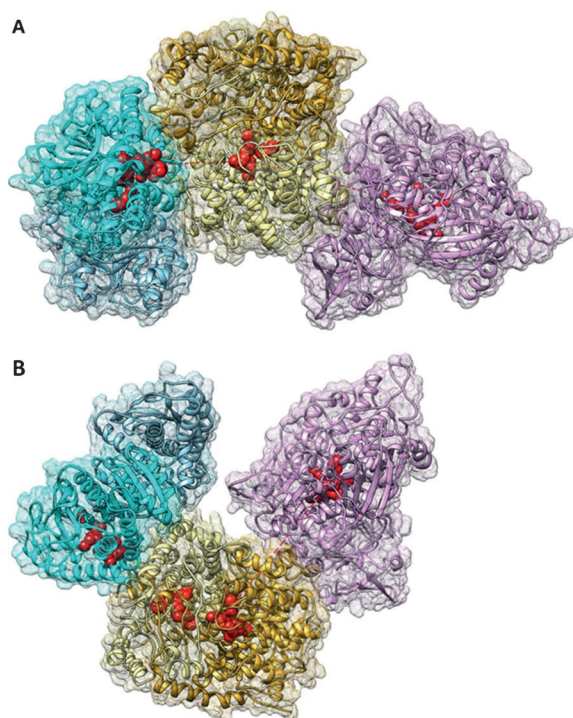

Figure 1. Two models, MCA1 (A) and MCA2 (B) of the mMDH-CS-ACON complex. The two chains of the CS homodimer are shown in gold and yellow. The two chains of mMDH homodimer are sky blue and cyan. ACON is a monomer is plum. Identified cross-links are represented by red bars with linked lysine residues numbered. C) Model of mMDH-CS complex before docking ACON. Crystal structures (mMDH: 1MLD; CS: 1CTS; ACON: 7ACN) from www.pdb.org were used for making models.

identified between mMDH Lys300, Lys304 and CS Lys 432, 437. Distance measurements revealed that the following residues are in very close proximity (less than 20 Å): mMDH Ile34–Pro38, Tyr56–Glu60, Gly77–Thr95, Lys215–Ala220 and CS Ser2–His28, Ser424–Lys437, suggesting that one C-terminal and one N-terminal of CS participate in forming the binding interface.
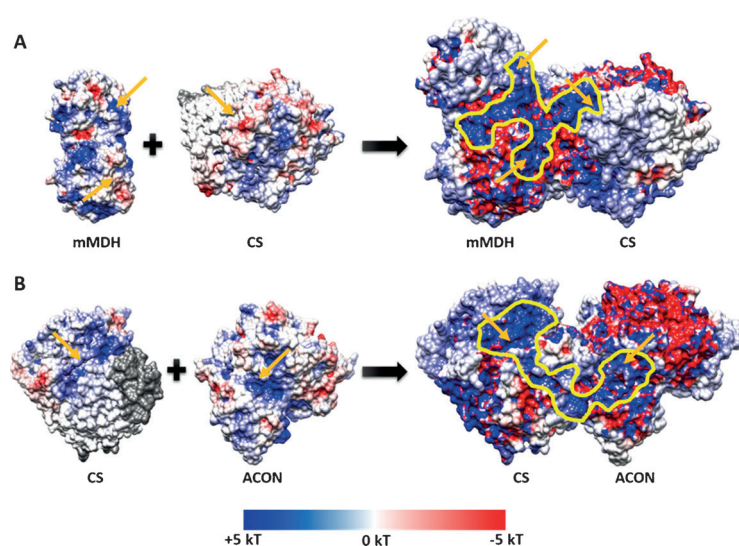
Docking ACON to CS was performed in the presence of mMDH. As indicated by our protein identification result, we assumed that CS has more affinity for mMDH than for ACON, and prefers to associate with mMDH. Therefore, the presence of mMDH may affect ACON's exploring the surface of CS. Assuming that the stoichiometric ratio was 1:1:1, we proposed two models for mMDH-CS-ACON complex. Illustrated in Figure 1A, ACON binds the same CS subunit as mMDH does. Four cross-links were identified between ACON Lys30, Lys201, Lys709 and CS Lys294, Lys300. There is also another possibility that ACON and mMDH are located on opposite sides as in model MCA2 (Figure 1B). Change of position does not cause increased separation of mMDH and ACON. On the contrary, their distance is dramatically shortened and the closest amino acids are within only 15 Å. Enhanced association between mMDH and ACON, however, led to a slightly loosened connection between CS and ACON. Only two cross-links were identified between ACON Lys30, Lys709 and CS Lys294, Lys300. Nonetheless, in both models, the C-terminus as well as the following regions of ACON were found to interact with the same residues on CS: ACON Asp48–Glu54, Phe544–Asp551, Leu702–Ala706, Glu733–Lys754, and CS Arg195–Ser199, CS Gly218–Asp221, CS Thr286–Val296, CS Pro342–Pro345, and CS Gly386–Asn391. No potential cross-links between mMDH and ACON were identified in either MCA1 or MCA2.

Forming complexes definitely brings enzyme active sites in close proximity, reducing diffusion lengths for substrates (Figure 2). The average distances between active sites are about 35 Å for mMDH-CS and 50 Å for ACON-CS in MCA1. Docking mMDH and ACON onto different subunits of CS resulted in increased active site separation to 65 Å for ACON–CS, and it seems less favorable for efficient substrate transport than MCA1 where mMDH and ACON are separated by only one active center. Comparing the binding surface areas (buried solvent accessible areas), MCA1, which has 10000 Å^2 for mMDH–CS and 13000 Å^2 for ACON–CS, is more thermodynamically favorable than MCA2, which has 10000 Å^2 for mMDH–CS and 12000 Å^2 for ACON–CS.

A theoretical study done by Elcock and McCammon demonstrated that the presence of surface electrostatic forces resulted in one order of magnitude increase in substrate-transport efficiency, while less than 1% of molecules are directly transported without electrostatic forces.[3a] In our study, by studying the surface electrostatic potentials of the metabolon structures, we were able to illustrate the charge redistribution upon association (Figure 3). Free CS is slightly negative while mMDH and ACON carry more positive charges at pH 7.8 (pH of mitochondrial matrix).
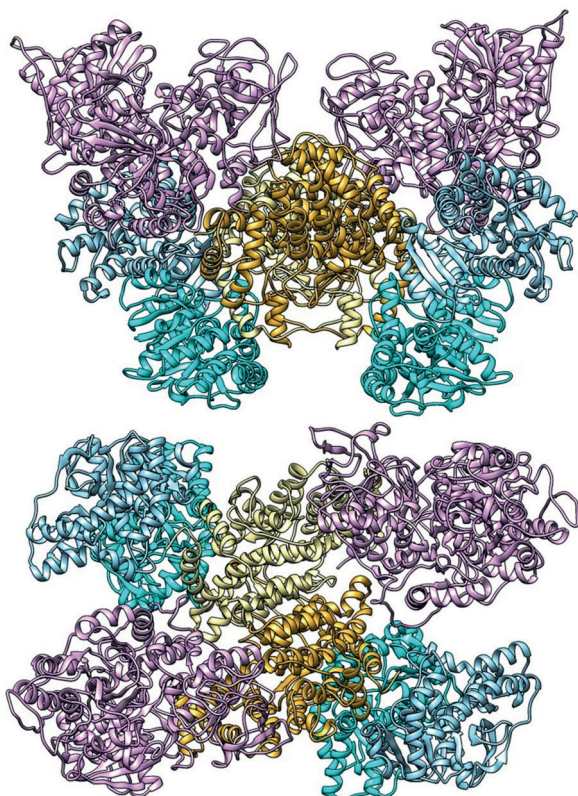

Figure 3. Illustration of surface electrostatic potential (ESP) on MCA1 and free enzymes at pH 7.8. A) Rearrangement of surface charge upon mMDH-CS complex formation. B) Rearrangement of surface charge upon CS-ACON complex formation. Active sites are denoted by orange arrows and electrostatic channels are highlighted by yellow edges. Negatively charged regions are red, positively charged are blue, and neutral regions are white.

Positively charged patterns around the active sites will facilitate accommodating substrates carrying negative charges. After docking, these patterns get expanded across binding interfaces and interconnected to form a continuous band (channel) linking active sites. In the meantime, negative charges have also been rearranged to cover regions next to the "channel" of positive potential. Under the combined effects of electrostatic attraction and repulsion, the traveling path and the time required for charged intermediates to reach the next active sites would be reduced, thus increasing transport efficiency and metabolic flux. Most buried residues are less polar and even hydrophobic. Involvement of different types of amino acids indicates that the complex is a balanced outcome of both electrostatic and hydrophobic interactions.

Finally, we constructed a higher-order model for the mMDH-CS-ACON complex based on MCA1, the more abundant structure. As shown in Figure 4, the central core, the CS dimer, is surrounded by two mMDH dimers and two ACON monomers. In this octamer, a two-fold symmetry is achieved. Each asymmetric subunit, composed of one CS subunit, one mMDH dimer, and one ACON monomer, is symmetric to the other.

In this study, we have experimentally demonstrated the existence of the Krebs cycle metabolon by identifying all eight enzymes through in vivo cross-linking and mass spectrometry. Using distance constraints derived from cross-links, we propose two models for the wild-type mMDH-CS-ACON complex and a two-fold symmetric octamer composed of two mMDH dimers, one CS dimer, and two ACON monomers. Analysis of surface electrostatic potential of our model shows that rearrangement of surface charge patterns upon protein–protein association leads to forming a continuous positively charged zone across their interface. This would consequently facilitate directed transport of negatively charged substrates

Figure 2. Illustration of active sites (red spheres) in MCA1 (A) and MCA2 (B). Active sites in mMDH are Ile12, Arg80, Arg86, Asn118, Arg152, and His176.[11] Active sites in CS are His238, Asn242, His274, and Arg401.[12] Active sites in ACON are His101, Asp165, Ser166, His167, Cys358, Arg447, Arg452, Ser642, Ser643, and Arg644.[13] Red dashed line represents the Euclidean distance. Meshed surface of the complex is also shown.

Figure 4. Two views of the octamer model of the mMDH-CS-ACON complex. Top: The two-fold symmetry axis is parallel to the plane and passes through the center of CS dimer. Bottom: The two-fold symmetry axis is perpendicular to the plane and points from the center of CS.

from one active site to the next. Until this work, direct observation of substrate channeling remained a big hurdle in metabolon research even though simulation work has built a theoretical foundation for achieving similar surface electrostatic complementarity with rational design of multi-enzyme complexes. Our investigation of natural Krebs cycle metabolons gains structural insight into the organization of wild-type enzymes within the mitochondrial matrix, and provides

an orientation option (MCA1) for the artificial metabolon formation. This information will help researchers in biocatalysis take a further step in the reconstruction of artificial metabolons of enzyme cascades in the desired orientation to achieve substrate channeling similar to that of natural metabolons.

[1] A. R. Fernie, F. Carrari, L. J. Sweetlove, *Curr. Opin. Plant Biol.* **2004**, *7*, 254–261.

[2] a) J. J. B. Robinson, L. Inman, B. Sumegi, P. A. Srere, *J. Biol. Chem.* **1987**, *262*, 1786–1790; b) J. J. B. Robinson, P. A. Srere, *J. Biol. Chem.* **1985**, *260*, 10800–10805; c) J. Ovádi, P. A. Srere, *Int. Rev. Cytol.* **2000**, *192*, 255–280; d) P. A. Srere, *Annu. Rev. Biochem.* **1987**, *56*, 255–280; e) P. A. Srere, B. Sumegi, A. D. Sherry, *Biochem. Soc. Symp.* **1987**, *54*, 173–182.

[3] a) A. H. Elcock, J. A. McCammon, *Biochemistry* **1996**, *35*, 12652–12658; b) I. Morgunov, P. A. Srere, *J. Biol. Chem.* **1998**, *273*, 29540–29544; c) K. Shatalin, S. Lebreton, M. Rault-Leonardon, C. Vélot, P. A. Srere, *Biochemistry* **1999**, *38*, 881–889; d) B. S. J. Winkel, *Annu. Rev. Plant Biol.* **2004**, *55*, 87–107.

[4] M. J. Moehlenbrock, T. K. Toby, A. Waheed, S. D. Minteer, *J. Am. Chem. Soc.* **2010**, *132*, 6288–6289.

[5] S. Schoffelen, J. C. M. v. Hest, *Soft Matter* **2012**, *8*, 1736–1746.

[6] C. Vélot, M. B. Mixon, M. Teige, P. A. Srere, *Biochemistry* **1997**, *36*, 14271–14276.

[7] A. Sinz, *Mass Spectrom. Rev.* **2006**, *25*, 663–682.

[8] A. E. Lyubarev, B. I. Kurganov, *BioSystems* **1989**, *22*, 91–102.

[9] S. F. D'Souza, P. A. Srere, *Biochim. Biophys. Acta Bioenerg.* **1983**, *724*, 40–51.

[10] a) S. F. D'Souza, P. A. Srere, *J. Biol. Chem.* **1982**, *258*, 4706–4709; b) T. Barnard, B. A. Afzelius, D. Lindberg, *J. Ultrastruct. Res.* **1971**, *34*, 544–566.

[11] W. B. Gleason, Z. Fu, J. Birktoft, L. Banaszak, *Biochemistry* **1994**, *33*, 2078–2088.

[12] S. Remington, G. Wiegand, R. Huber, *J. Mol. Biol.* **1982**, *158*, 111–152.

[13] H. Lauble, M. C. Kennedy, H. Beinert, C. D. Stout, *Biochemistry* **1992**, *31*, 2735–2748.